

Identifying spatial interaction zones between humans and long-tailed macaques in the Mount Merbabu landscape, Indonesia

NURPANA SULAKSONO¹, IKE NURJUITA NAYASILANA^{2,*}, YAYAN HADIYAN³,
SUBYANTORO TRI PRADOPO⁴, ANGGIT HARYOSO¹, JAROT WAHYUDI¹,
DHANA PUSPITA ADININGTYAS², RIZKI ANDIKA PUTRA²

¹Gunung Merbabu National Park, Ministry of Forestry, Republic of Indonesia. Jl. Merbabu 136, Boyolali 57316, Central Java, Indonesia

²Program of Forest Management, Faculty of Agriculture, Universitas Sebelas Maret. Jl. Ir. Sutami 36A, Surakarta 57126, Central Java, Indonesia.

Tel./fax.: +62-271-637457 Ext. 129, *email: nayasilana@staff.uns.ac.id

³Research Center for Ecology, National Research and Innovation Agency (BRIN). Jl. Raya Bogor KM. 46, Cibinong, Bogor 16911, West Java, Indonesia

⁴Gunung Merapi National Park, Ministry of Forestry, Republic of Indonesia. Jl. Kaliurang KM. 22.6, Sleman 55582, Yogyakarta, Indonesia

Manuscript received: 25 January 2026. Revision accepted: 10 April 2026.

Abstract. Sulaksono N, Nayasilana IN, Hadiyan Y, Pradopo ST, Haryoso A, Wahyudi J, Adiningtyas DP, Putra RA. 2026. Identifying spatial interaction zones between humans and long-tailed macaques in the Mount Merbabu landscape, Indonesia. *Biodiversitas* 27 (4): d270414. <https://doi.org/10.13057/biodiv/d270414>. Human-long-tailed macaque (*Macaca fascicularis*) interactions are an increasing conservation and management concern in Indonesia, particularly within forest-agriculture-settlement mosaics surrounding protected areas. This study aimed to identify spatial interaction zones between humans and long-tailed macaques using habitat suitability modeling in the Mount Merbabu landscape. Habitat suitability was modeled using the Maximum Entropy (MaxEnt) algorithm based on occurrence records from direct field encounters and indirect evidence of macaque presence. Model complexity was optimized using the ENMeval framework based on the Akaike Information Criterion corrected for small sample sizes (AICc), cross-validated AUC, and omission rate. Eight environmental and anthropogenic predictors representing topography, vegetation, disturbance, and human proximity were included in the model. The final model showed stable predictive performance (cross-validated AUC: 0.7469±0.1023). Distance to burned areas emerged as the strongest predictor, followed by distance to settlements and land cover. Suitable habitat covered 4,131.71 ha (25.80%) of the interaction analysis area (16,010.88 ha) outside the national park and extended beyond forest interiors into surrounding agricultural and settlement landscapes. Moderate and high interaction zones (3,511.44 ha and 620.28 ha, respectively) formed localized clusters along forest-agriculture transition areas surrounding the national park. Sensitivity analysis showed that the spatial configuration of interaction zones remained consistent across alternative occurrence models. These mapped zones represent relative spatial interaction potential derived from macaque occurrence patterns and their overlap with human land use, rather than direct predictions of conflict incidence. The results demonstrate that MaxEnt-based spatial modeling provides a useful framework for identifying potential human-wildlife interaction zones and supporting spatially targeted mitigation in protected-area buffer landscapes.

Keywords: Disturbance ecology, human-primate interactions, *Macaca fascicularis*, MaxEnt, species distribution modeling

INTRODUCTION

Human-wildlife conflict (HWC) is an increasingly pervasive challenge in landscapes where protected habitats intersect with expanding human land use (Anand and Radhakrishna 2017). Across many regions, rapid land-use change (particularly forest conversion, agricultural expansion, and intensified human activities) has amplified spatial overlap between wildlife habitats and human livelihoods (Soulsbury and White 2015; Ji et al. 2022; Larson et al. 2023). These conflicts often emerge where competition for space and resources intensifies along human-ecological interfaces (Matseketsa et al. 2019). Such interactions can result in crop losses, threats to human safety, and retaliatory responses toward wildlife, posing challenges for biodiversity conservation in human-dominated landscapes (Anand and Radhakrishna 2017; Sharma et al. 2020). Among human-wildlife interactions, conflicts involving primates have become increasingly prominent, particularly those associated with the long-tailed macaque (Fratesi et al.

2026). Across Southeast Asia, this species has frequently been reported as a source of human-primate conflict in urban areas, agricultural landscapes, tourism sites, and settlements (Yeo and Neo 2010; Mishra et al. 2020; Entezami et al. 2024; Rifaie et al. 2024). These conflicts commonly involve crop raiding, property damage, and aggressive encounters with humans (Syah 2020, Entezami et al. 2024). The species' behavioral flexibility allows it to exploit human-modified landscapes, increasing the frequency of human-macaque interactions (Koirala et al. 2022).

Despite growing research on human-long-tailed macaque conflict, spatially explicit approaches that distinguish between reported conflict events and landscapes predisposed to future interaction remain limited (Fitria et al. 2020; Koirala et al. 2022). Reported incidents may underestimate broader landscape-level risk due to reporting bias, whereas habitat suitability models may overestimate conflict potential when social and behavioral factors are not considered. Identifying spatial interaction zones, where suitable wildlife habitat overlaps with human land use, provides a framework for

assessing potential conflict areas as spatial risk rather than documented events. In this study, interaction zones are defined as areas outside the national park where predicted macaque habitat suitability exceeds the threshold and intersects with human-dominated land uses, particularly agriculture and settlements. Species distribution modeling using the Maximum Entropy (MaxEnt) algorithm provides a widely used approach to estimate habitat suitability from presence-only occurrence data and environmental predictors (Phillips and Dudík 2008; Elith et al. 2011). By integrating predicted suitability with human land use, MaxEnt helps identify spatial interaction zones for mitigation prioritization (Zvidzai et al. 2023; Syahrani et al. 2025). These predictions represent relative habitat suitability rather than direct conflict events.

In this study, spatial interaction potential is conceptualized as the landscape context where wildlife occurrence overlaps with human land use. Occurrences provide evidence of macaque presence within the landscape and, when integrated with environmental predictors, enable habitat suitability models to estimate the relative likelihood of occurrence across environmental gradients (Phillips and Dudík 2008; Elith et al. 2011). However, occurrence data may reflect spatial sampling or reporting bias. When areas of high predicted suitability overlap with human-dominated land uses such as agriculture and settlements, the likelihood of spatial encounters between humans and macaques increases (Nyhus 2016; Koirala et al. 2022). However, habitat suitability reflects relative environmental conditions rather than population density or realized human-wildlife interactions. This framework, therefore, represents relative spatial interaction potential while acknowledging that social and behavioral factors influencing realized conflict outcomes are not explicitly modeled.

This study advances human-wildlife conflict research by shifting the analytical focus from observed conflict hotspots to landscape-level predisposed risk through the delineation of human-wildlife interaction zones. The analysis incorporates fire legacy, represented by distance to burned areas, as a disturbance-related factor that can alter vegetation structure, resource availability, and habitat configuration, thereby influencing wildlife movement patterns and the likelihood of interactions in post-fire landscapes (Neves et al. 2020; Santosa and Kwatrina 2020). In addition, a sensitivity comparison between confirmed occurrence (CO) and indirect occurrence models (IOM) is conducted to evaluate how alternative occurrence datasets influence interaction-potential mapping. This study applies MaxEnt modeling to estimate habitat suitability for long-tailed macaques and delineate spatial interaction zones with human land use in the Mount Merbabu landscape surrounding Gunung Merbabu National Park (GMNP), while evaluating the robustness of these predictions using alternative occurrence datasets to support early-stage conflict mitigation and conservation planning.

MATERIALS AND METHODS

Study area

The research was conducted in the Mount Merbabu landscape, encompassing Gunung Merbabu National Park (GMNP) and adjacent human-dominated areas that border the park. Administratively, the study area spans the districts of Magelang, Semarang, and Boyolali in Central Java, Indonesia. Geographically, the Mount Merbabu landscape is located between approximately 110°26'-110°30'E and 7°26'-7°30'S, with elevations ranging from about 533 to 3,126 m above sea level (Figure 1).

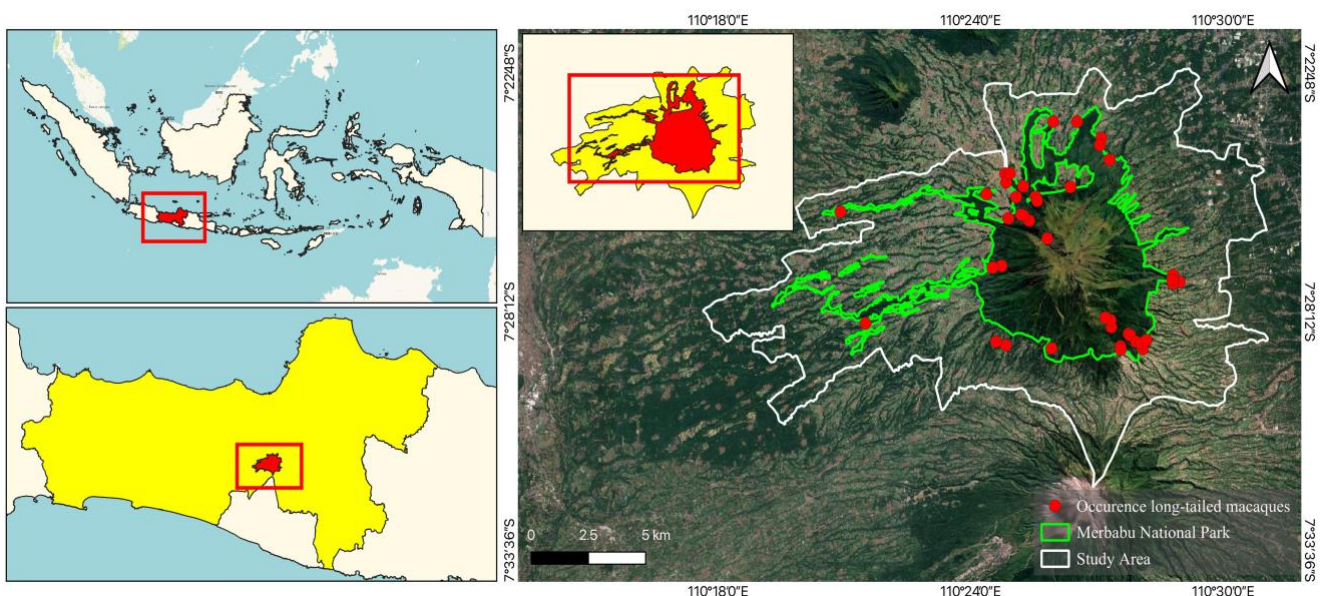


Figure 1. Location of the study area in the Mount Merbabu Landscape, Central Java, Indonesia, showing Gunung Merbabu National Park, the surrounding landscape, and long-tailed macaque occurrence records derived from direct observations and verified crop-damage reports from surrounding agricultural areas used in this study

The study area was delineated using the administrative boundaries of 36 villages directly adjacent to the national park (approximately 21,893 ha), representing the primary forest-agriculture-settlement interface where human-long-tailed macaque interactions are most prevalent. Although village boundaries do not represent ecological limits to macaque movement, they were used as an operational and management-relevant study extent because human-macaque interactions, reporting mechanisms, and mitigation actions are organized at the village level.

Three spatial extents were defined to clarify the analytical framework of this study. First, the full landscape extent (21,893 ha) represents the administrative boundaries of the 36 villages adjacent to GMNP. Second, this landscape extent was used as the accessible area (M) for MaxEnt calibration, approximating the area potentially accessible to macaques beyond the park boundary. Third, habitat suitability modeling was conducted across this accessible landscape extent. Finally, the delineation of human-macaque interaction zones was restricted to the human-dominated interaction-analysis area outside the national park (16,010.88 ha), where predicted habitat suitability overlaps with surrounding land uses.

The national park is dominated by lower and upper montane forests characterized by vegetation such as *Castanopsis*, *Lithocarpus*, and *Schima wallichii*, which support diverse wildlife, including primates and ungulates (Sawitri et al. 2010; Sari et al. 2018; Fadhillah 2020). Surrounding areas consist mainly of agricultural land, settlements, and nature-based tourism sites, forming a forest-agriculture-settlement mosaic where local communities rely on forest resources for grass harvesting, firewood, and water (Aissiyah et al. 2019; Esthi et al. 2022; Dewi et al. 2024). The Mount Merbabu ecosystem is highly dynamic and frequently influenced by recurrent fire disturbances that shape vegetation structure and landscape dynamics (Ardiaristo et al. 2024).

Occurrence data

Occurrence data were compiled from direct field observations and verified indirect evidence of long-tailed macaque activity. Direct observations were conducted using a line transect method within GMNP and along its boundary. A total of 8 transects were established, ranging from approximately 800 to 2,000 m in length. Each transect was surveyed twice during the field data collection period to increase the likelihood of detecting macaque groups.

For each macaque group encountered, a single geographic coordinate was recorded to represent the group's location, together with the number of individuals observed. Indirect records of macaque presence outside the national park were obtained from community-reported crop damage in agricultural areas, supported by physical evidence and official records from the GMNP authority. Verification involved interviews with affected farmers and park staff, complemented by field documentation and photographic evidence. Interviewees were selected purposively, focusing on farmers who had experienced crop damage caused by macaques and park staff familiar with conflict incidents in the area. Semi-structured interviews were conducted to

verify reported incidents using a standardized interview protocol. Interview questions covered (i) the location of crop-damage incidents, (ii) the frequency and timing of macaque visits, (iii) the types of crops affected, and (iv) observed macaque behavior during crop-raiding events. Information obtained from interviews was cross-checked with field observations, photographic documentation, and official reports from the GMNP authority to confirm incident validity. All verified indirect records were georeferenced and treated as confirmed locations of macaque occurrence or activity in human-dominated landscapes, indicating macaque use of surrounding agricultural landscapes.

A total of 56 occurrence records were initially compiled from both direct field observations and community-reported crop-damage incidents, indicating macaque activity. Prior to modeling, occurrence points were spatially thinned using a minimum distance of 100 m to reduce spatial autocorrelation and potential pseudo-replication associated with repeated detections of the same macaque group. This threshold was also consistent with the 30 m environmental raster resolution used in the analysis. After thinning, 45 spatially independent occurrence points were retained for modeling. Potential duplicate records between direct observations and community reports were screened based on spatial proximity and temporal correspondence. Overlapping records were consolidated into a single occurrence point. Repeated observations potentially associated with the same macaque group across different survey dates were also screened. Similarly, crop-damage reports originating from the same agricultural fields that experienced repeated raids were merged when occurring at the same or closely adjacent locations. Direct field surveys were conducted between August and September 2025, whereas official crop-damage reports used as indirect occurrence records covered the period from January to December 2025.

Given differences in detection and reporting processes between data sources, spatial bias, particularly clustering near accessible agricultural areas, may be present. Accordingly, model outputs are interpreted as relative patterns of macaque occurrence associated with environmental suitability and human-accessible landscapes. To evaluate the potential influence of alternative detection sources, a sensitivity analysis comparing models based on confirmed occurrence records (CO) and indirect occurrence models (IOM) was conducted. The CO model used the full dataset of spatially filtered occurrence records (n: 45), whereas the IOM model was calibrated exclusively using the subset of indirect occurrence records derived from community-reported crop-damage incidents (n: 26). The IOM therefore represents an alternative sampling lens based on incident reports, reflecting macaque activity filtered by human reporting opportunity and landscape accessibility. Accordingly, the response variable represents confirmed locations of macaque occurrence or activity rather than direct predictions of conflict probability or human-macaque interaction outcomes. Spatial interaction potential is derived only in a subsequent analytical step by overlaying predicted habitat suitability with human land-use areas outside the national park.

Environmental and disturbance variables

A suite of environmental and anthropogenic variables was compiled as candidate predictors to represent geographic, ecological, and human-related factors influencing wildlife distribution (Wu et al. 2024). Environmental predictors were derived from multi-temporal datasets to characterize baseline habitat conditions and disturbance dynamics. Vegetation and land-cover variables derived from 2024 imagery were assumed to represent landscape conditions during the 2025 occurrence surveys because land-use patterns in the Mount Merbabu landscape remain relatively stable over short time intervals. Burned-area data from 2023 were included to capture disturbance legacies that may influence vegetation structure and resource distribution beyond the year of fire occurrence. This temporal configuration was therefore considered analytically appropriate because land-cover and vegetation variables represent relatively stable habitat conditions, whereas burned-area data capture disturbance effects that may persist for several subsequent seasons.

The geographic predictors included slope, aspect, elevation, land cover, distance to dense forest, and distance to rivers, whereas anthropogenic variables comprised distance to settlements, agricultural areas, burned areas, and roads (Fauzi et al. 2020; Sharma et al. 2020) (Table 1). Topographic variables (slope, aspect, and elevation) were derived from the Shuttle Radar Topography Mission (SRTM) 1 Arc-Second Global dataset (Farr et al. 2007), accessed through Google Earth Engine (GEE). Vegetation conditions were represented by the Normalized Difference Vegetation Index (NDVI), generated from Landsat 8 Operational Land Imager Collection 2 Level-2 surface reflectance imagery acquired in 2024 (EROS Center 2020). Land-cover classification was conducted using Sentinel-2 Level-2A surface reflectance imagery from 2024 (European Space Agency 2021). Image processing and spatial analyses were implemented using the GEE platform (Safanelli et al. 2020).

Distance layers representing settlements, agricultural areas, and rivers were derived from the Indonesian Topographic Map (RBI) provided by the Geospatial Information Agency of Indonesia (Badan Informasi Geospasial 2019) and processed in QGIS version 3.16. All environmental predictors were standardized as raster layers with a spatial resolution of 30 m, and distance-based variables were calculated using Euclidean distance analysis (Wu et al. 2024). All spatial analyses were conducted in the WGS 1984 UTM Zone 49S coordinate system.

Burned areas were identified using Landsat 8 Operational Land Imager (OLI) Collection 2 Level-2 surface reflectance imagery acquired before (1 August-30 September 2023) and after (1 November-31 December 2023) the fire event (27-30 October 2023). Image processing was conducted in Google Earth Engine (GEE), with clouds and cloud shadows masked using the QA_PIXEL band. Burn severity was assessed using the differenced Normalized Burn Ratio (dNBR), calculated from pre- and post-fire NBR values derived from the near-infrared (NIR) and shortwave infrared (SWIR) bands (Lee et al. 2025). A threshold value of 0.300 (moderate burn severity) was applied following Lee et al. (2025) to delineate fire-affected areas. Burned area was treated as a legacy disturbance variable reflecting longer-term post-fire habitat alteration rather than a direct measure of fire pressure. The burned-area map was evaluated through visual inspection and spatial validation against independent active-fire detections from NASA FIRMS. Validation quantified the proportion of dNBR-derived burned area overlapping 375 m and 750 m buffers around FIRMS detections, representing the nominal VIIRS fire pixel size and an extended tolerance distance to account for geolocation uncertainty (Schroeder et al. 2014). Approximately 84.85% of the burned area (308.45 ha of 363.51 ha) overlapped the 375-m buffer, increasing to 99.48% (361.64 ha) within the 750-m buffer.

Table 1. Candidate environmental and anthropogenic predictor variables considered in habitat suitability modeling and their final status after multicollinearity screening

Predictor variable	Data type	Source	Variable status
Environmental factors			
Aspect	Continuous	Shuttle Radar Topography Mission (SRTM) 1 Arc-Second Global	Retained
Slope	Continuous	Shuttle Radar Topography Mission (SRTM) 1 Arc-Second Global	Retained
Land cover	Categorical	Sentinel-2A imagery (2024)	Retained
Elevation	Continuous	Shuttle Radar Topography Mission (SRTM) 1 Arc-Second Global	Removed (collinearity)
NDVI	Continuous	USGS Landsat 8 Level-2, Collection 2, Tier 1 (2024)	Retained
Distance to rivers (DistRiver)	Continuous	Indonesian Topographic Map (RBI)	Retained
Distance to dense forest (DistForest)	Continuous	Sentinel-2A imagery (2024)	Retained
Disturbance factors			
Distance to burned areas (DistBurnArea)	Continuous	USGS Landsat 8 Level-2, Collection 2, Tier 1 (2023)	Retained
Distance to roads (DistRoad)	Continuous	Indonesian Topographic Map (RBI)	Removed (collinearity)
Distance to settlements (DistSettle)	Continuous	Indonesian Topographic Map (RBI)	Retained
Distance to agricultural areas (DistFarm)	Continuous	Indonesian Topographic Map (RBI)	Removed (collinearity)

Land-cover mapping was performed using the GEE platform with Sentinel-2 Level-2A surface reflectance imagery from 2024 as the primary data source (Pérez-Cutillas et al. 2023; Lee et al. 2025). Four land-cover classes were defined (Forest, Agriculture, Built-up, and Grassland) at a coarse structural level, based on canopy cover and structural characteristics rather than vegetation species composition, given the high heterogeneity of vegetation types in the Mount Merbabu landscape and the spatial resolution of the imagery (Table 2). In subsequent land-use overlay analyses, the Mount Merbabu National Park area was excluded. The “forest” class therefore refers only to forest outside the park boundary, including community forests, secondary forests, and other non-park forest patches (Table 2). Classification was conducted using the Random Forest algorithm in GEE, with Sentinel-2 spectral bands as predictors (Ardiaristo et al. 2024).

Training and validation samples were generated by visual interpretation, using a combination of high-resolution imagery and Sentinel-2 multispectral bands to ensure accurate identification of surface features. Sample selection followed a stratified approach across land-cover classes to ensure balanced class representation. A total of 435 reference samples were used, with 292 samples used for model training and 143 independent samples used for validation, corresponding to the dataset used to construct the confusion matrix (Table 3 and Table 4). Visual interpretation was further informed by the authors’ long-term field experience in the study landscape, which was used to support interpretation consistency rather than as an unstructured subjective judgment, ensuring reliable identification of land-cover structures relevant to wildlife habitat modeling.

Table 2. Operational definitions and visual interpretation rules used to classify land-cover types in the Mount Merbabu landscape. Four classes (forest, agriculture, built-up, and grassland) were identified based on dominant surface characteristics and interpreted visually from satellite imagery using key elements such as color tone, texture, pattern, and landscape context

Land-cover class	Operational definition	Visual interpretation rules (ocular interpretation)
Forest	Areas dominated by continuous tree canopy forming closed or semi-closed forest cover, including primary and secondary forest	Dark to medium green appearance, dense and heterogeneous texture; irregular patch shape, continuous canopy without visible field boundaries, commonly associated with higher elevation zones
Agriculture	Cultivated land including cropland, mixed agriculture, and smallholder plantations	Regular or semi-regular geometric patterns, visible field boundaries; patchy texture; seasonal variation in color tone, frequently adjacent to settlements or access roads
Built-up	Human-constructed surfaces such as settlements, facilities, and road networks	Bright gray to whitish appearance, very coarse and heterogeneous texture; linear or block-like patterns, sharp contrast with surrounding land cover
Grassland	Open areas dominated by grasses or low herbaceous vegetation with limited woody cover, including montane savanna with sparse tree cover.	Light green to brownish appearance, smooth and homogeneous texture; open patches without tree canopy, often occurring on ridges, slopes, or disturbed areas

Table 3. Number of training and validation samples per land-cover class

Land-cover class	Training samples (n)	Validation samples (n)	Total samples (n)
Built-up	76	35	111
Agriculture	80	42	122
Forest	69	32	101
Grassland	67	34	101
Total	292	143	435

Table 4. Accuracy assessment of the land-cover classification based on validation samples. The table presents producer’s accuracy and user’s accuracy for each land-cover class, along with the overall classification accuracy and Kappa coefficient derived from the confusion matrix

Land-cover class	Validation samples (n)	Producer’s accuracy (%)	User’s accuracy (%)
Built-up	35	100	94.59
Agriculture	42	95.24	97.56
Forest	32	100	96.97
Grassland	34	93.94	96.88
Overall accuracy	-	96.5	-
Kappa coefficient	-	0.953	-

Classification accuracy was evaluated using a confusion matrix derived from independent validation samples, from which overall accuracy, the Kappa coefficient, and class-specific producer's and user's accuracy were calculated (Table 4). The classification achieved an overall accuracy of 96.5% with a Kappa coefficient of 0.953, indicating strong agreement between classified and reference data. The resulting land-cover layer was interpreted as a representation of prevailing land-use and vegetation structure rather than year-specific dynamics and was used to quantify the spatial distribution of land-cover classes across the Mount Merbabu landscape.

Data pre-processing, multicollinearity analysis, and variable selection

To assess multicollinearity among predictor variables, a Pearson correlation test was conducted on ten continuous candidate variables using 1,000 randomly sampled points within the modeling mask (accessible area, M) used for MaxEnt calibration (Chai et al. 2016). The accessible area (M) represented the landscape potentially accessible to macaques beyond the park boundary and was operationally defined by merging the national park boundary with the administrative boundaries of surrounding villages included in the Mount Merbabu landscape. Categorical variables such as land cover were excluded because Pearson's correlation is not appropriate for nominal data. The correlation analysis was performed on the GEE platform, and the results are presented in Table 5. A correlation threshold of $|R| > 0.7$ was applied (Dormann et al. 2013), as values above this level are commonly considered indicative of strong correlation and potential multicollinearity. For highly correlated variables, one predictor was retained based on ecological relevance and interpretability. As a result, elevation, distance to roads, and distance to agricultural areas were excluded from further analysis. Elevation was removed due to strong collinearity with climate- and vegetation-related variables; ecologically, it acts as a proxy for these gradients rather than an independent driver, and its signal was therefore retained indirectly through correlated predictors.

The final MaxEnt model retained eight predictor variables, including distance to burned areas, distance to rivers, distance to settlements, distance to dense forest, and

environmental variables comprising aspect, slope, NDVI, and land-cover classes (Figure 2). Although land cover, NDVI, and distance to dense forest may partially overlap conceptually, they represent different ecological dimensions of macaque habitat use, capturing complementary aspects of vegetation structure, productivity, and proximity to refuge habitat. Land cover reflects the structural characteristics of the landscape. NDVI represents vegetation productivity and greenness, commonly used as a proxy for habitat quality and vegetation availability influencing mammal distribution (Osman et al. 2022). Distance to dense forest indicates proximity to continuous forest habitat that may provide refuge, sleeping sites, and movement corridors for macaque groups (Johnson et al. 2020). Together, these predictors represent complementary ecological dimensions of habitat suitability rather than redundant vegetation information.

Model evaluation, threshold selection, sensitivity analysis

Habitat suitability and spatial interaction potential were modeled using the Maximum Entropy algorithm implemented in MaxEnt version 3.4.4 (Phillips et al. 2006; Phillips and Dudík 2008). Model complexity was optimized using the ENMeval package in R by evaluating combinations of feature classes and regularization multipliers ranging from 0.5 to 4.0 (Muscarella et al. 2014; Kass et al. 2021). Candidate models were calibrated using spatial block cross-validation to reduce the influence of spatial autocorrelation and uneven sampling. Model performance was evaluated using Akaike Information Criterion corrected for small sample sizes (AICc), complemented by validation Area Under the Curve (AUC) and omission rate at the minimum training presence threshold (MTP) (Muscarella et al. 2014; Kass et al. 2021).

A total of 10,000 background points were randomly sampled within the accessible Mount Merbabu landscape. To reduce potential sampling bias arising from heterogeneous detection processes (systematic transects and conflict reports), spatial thinning and spatial block cross-validation implemented in ENMeval were applied, which have been shown to partially mitigate bias in presence-only modeling (Phillips et al. 2009; Elith et al. 2011).

Table 5. Pairwise-Pearson correlation coefficients among continuous predictors used for multicollinearity screening prior to MaxEnt modeling

Variable	Aspect	Elevation	DistForest	DistRoad	DistBurnArea	DistFarm	NDVI	DistSettle	Slope	DistRiver
Aspect	1.00	0.01	0.05	-0.02	0.22	-0.01	-0.01	0.03	0.02	-0.12
Elevation	0.01	1.00	0.12	0.79	-0.73	0.75	0.02	0.85	0.60	-0.03
DistForest	0.05	0.12	1.00	0.07	-0.02	0.11	-0.64	0.09	-0.09	0.22
DistRoad	-0.02	0.79	0.07	1.00	-0.45	0.94	0.12	0.92	0.52	-0.05
DistBurnArea	0.22	-0.73	-0.02	-0.45	1.00	-0.39	-0.03	-0.44	-0.46	-0.04
DistFarm	-0.01	0.75	0.11	0.94	-0.39	1.00	0.05	0.92	0.42	-0.01
NDVI	-0.01	0.02	-0.64	0.12	-0.03	0.05	1.00	0.10	0.22	-0.18
DistSettle	0.03	0.85	0.09	0.92	-0.44	0.92	0.10	1.00	0.55	-0.02
Slope	0.02	0.60	-0.09	0.52	-0.46	0.42	0.22	0.55	1.00	-0.10
DistRiver	-0.12	-0.03	0.22	-0.05	-0.04	-0.01	-0.18	-0.02	-0.10	1.00

Note: Values in bold denote high correlations ($R > 0.7$)

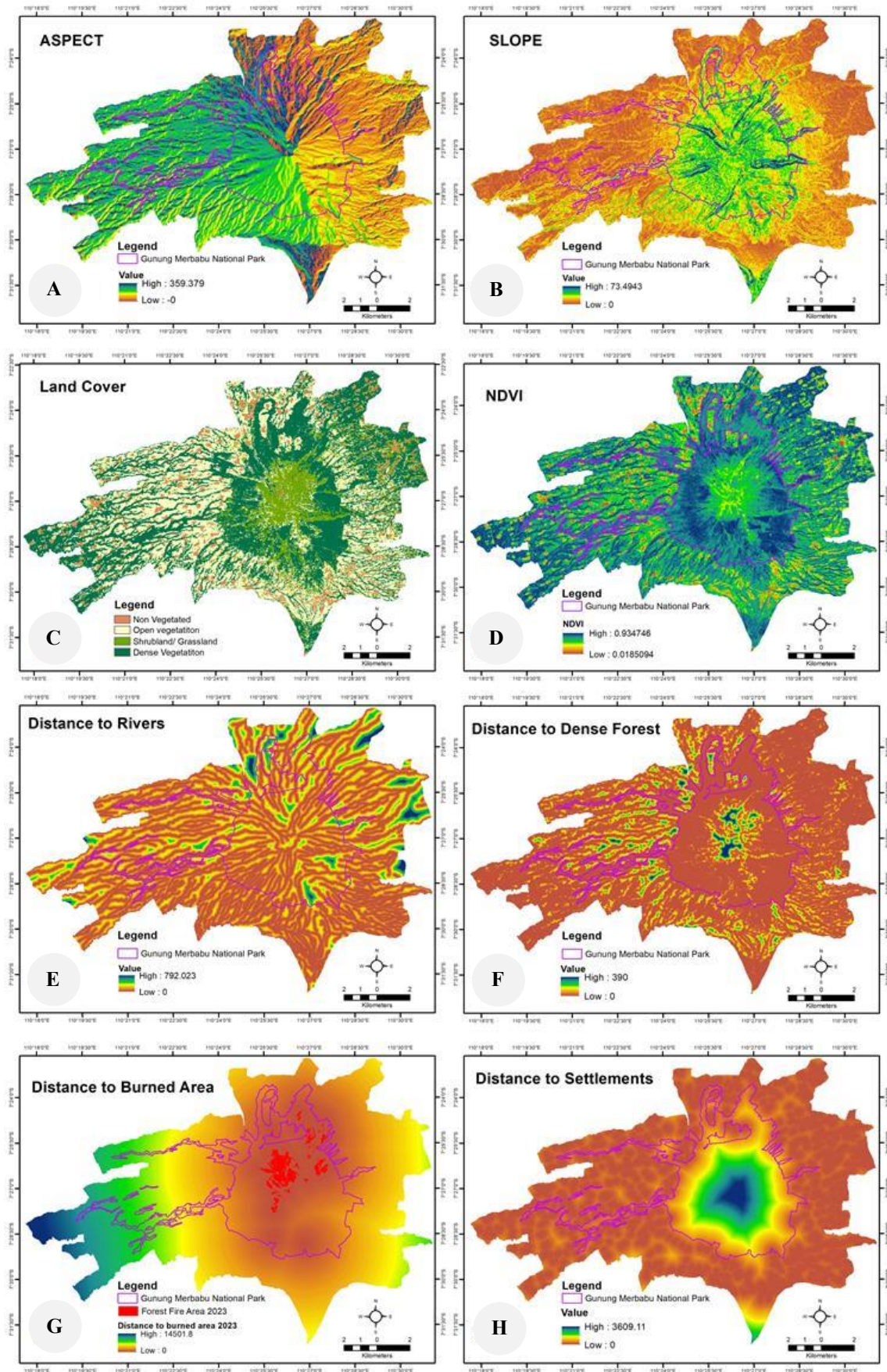


Figure 2. Map of environmental and disturbance predictors used as input layers in the MaxEnt modeling framework. A. aspect, B. slope, C. land cover, D. NDVI, E. distance to rivers, F. distance to dense forest, G. distance to burned area, H. distance to settlements

Habitat suitability was expressed using the cloglog output format, with clamping and extrapolation enabled. Explicit bias files or target-group background were not applied; instead, spatial block cross-validation within the ENMeval framework served as the primary strategy to reduce spatial clustering and uneven sampling arising from mixed data sources (transect surveys and conflict reports). The optimal parameter configuration selected by ENMeval consisted of feature class LQ with a regularization multiplier of 4, which was implemented in the final MaxEnt model, while all other parameters not included in the tuning procedure were retained at their default settings.

Habitat suitability thresholds were determined using the Maximum Training Sensitivity plus Specificity (MTSS) criterion (Li et al. 2024; Tang et al. 2025). The MTSS value derived from the MaxEnt cloglog output was used to separate unsuitable ($< \text{MTSS}$) and suitable ($\geq \text{MTSS}$) environmental conditions (Table 6). Spatial interaction zones were subsequently derived by intersecting suitable habitat with human-dominated land-use areas located outside the national park boundary to identify areas where macaque habitat suitability overlaps with human land use. Within this area, relative interaction potential was classified using a quantile-based approach. Pixels exceeding the 75th percentile of predicted suitability were categorized as high interaction potential and the remaining suitable pixels were classified as moderate interaction potential. This two-step framework separates environmental suitability from relative interaction potential and is intended for spatial prioritization rather than representing ecological thresholds or observed conflict probability. The resulting classes (moderate and high) therefore represent relative prioritization categories rather than biologically validated thresholds of conflict severity.

To translate these pixel-based interaction potential classes into spatially explicit management units, the classified interaction potential raster was subsequently integrated with ancillary spatial datasets. Specifically, the interaction potential map was spatially overlaid with land-use data across the interaction-analysis area outside the national park, including forest patches, agricultural land, grassland, and settlements, followed by a protected-area exclusion process to remove national park areas from further analysis. The resulting raster was overlaid with village administrative boundaries to calculate the total area (ha) of each interaction class within each village. The analytical workflow used to derive these spatial interaction potentials is summarized in Figure 3. Operationally, spatial interaction zones were defined as, Interaction zone = suitable habitat \cap human-dominated land use \cap outside the national park. Where, \cap denotes spatial intersection among raster layers where \cap denotes spatial intersection among raster layers

Subsequently, a sensitivity analysis was conducted to evaluate the extent to which variations in input data influence model outputs, thereby assessing the stability and reliability of the modeling results. Two alternative model configurations were compared. The CO model was developed using all available occurrence records, including both direct field observations and indirect evidence. In contrast, the IOM model was constructed exclusively from indirect occurrence records derived from community-reported conflict incidents, which were predominantly located outside the national park boundary, mainly in agricultural areas. To ensure methodological consistency, the sensitivity analysis was performed using the same modeling framework as the primary model, including the identical MaxEnt software application, environmental predictor variables, and optimized model parameter settings derived from ENMeval tuning.

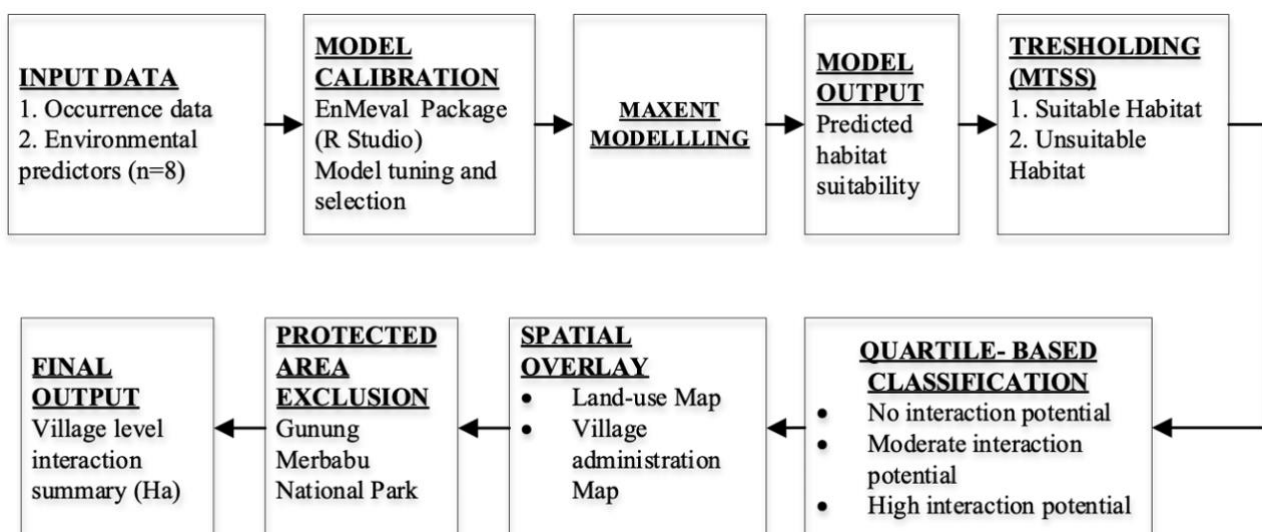


Figure 3. Workflow for habitat suitability modeling and spatial interaction potential delineation. Habitat suitability was modeled using MaxEnt and thresholded using the MTSS criterion. Suitable areas were further classified into interaction potential classes using a quartile-based approach. Interaction potential was spatially overlaid with land-use data, followed by protected-area exclusion of national park boundaries. The resulting interaction potential was summarized at the village level

Table 6. Threshold-based classification of relative human-long-tailed macaque spatial interaction zones outside the national park. Interaction potential classes were derived from MaxEnt habitat suitability using the MTSS threshold and the 75th percentile (Q_{75}) of predicted suitability values

Habitat suitability	Potential interaction class	Threshold (cloglog)	Description
Unsuitable	No interaction potential	<0.558	Areas outside the national park with suitability values below the MTSS threshold, indicating unsuitable environmental conditions for consistent macaque presence and negligible spatial interaction potential.
Suitable	Moderate interaction potential	0.558-0.808	Areas exceeding the MTSS threshold but remaining below the 75th percentile of predicted suitability, indicating suitable conditions with moderate spatial interaction potential.
	High interaction potential	>0.808	Areas exceeding the 75th percentile of predicted suitability, indicating relatively high habitat suitability and elevated potential for human-macaque spatial interaction.

The IOM model differed from the CO model only in the occurrence data used, while all other components of the modeling procedure remained constant. Model sensitivity was assessed by comparing model performance metrics (AUC, gain, and omission rate), variable contribution (percent contribution), and spatial outputs, including changes in the extent and spatial distribution of predicted suitable habitat. Threshold values used to delineate spatial interaction zones were calculated independently for each model to ensure that comparisons reflected differences in occurrence data rather than threshold transfer between models.

RESULTS AND DISCUSSION

Occurrence records and crop-damage observations of long-tailed macaques

A total of 45 occurrence points were compiled for analysis, consisting of 19 direct field observations within and along the boundary of GMNP and 26 validated indirect records derived from community-reported crop damage outside the national park. After spatial screening and thinning, these records formed the basis for the habitat suitability modeling. Most records were located within GMNP, where 19 macaque groups totaling 196 individuals were observed, with group sizes ranging from 3 to 18 individuals. Macaques at the study site have not undergone intensive habituation to humans and generally display avoidance behavior when encountering people, in contrast to more habituated populations where aggressive encounters are more common (Syah 2020). Most encounters occurred in forested areas of GMNP, with only occasional use of agricultural and transitional land-use zones as temporary foraging areas. Consequently, crop damage occurring along the forest edge suggests that conflict is driven by spatial proximity between natural habitats and anthropogenic food sources, rather than by direct interactions within residential areas. This spatial pattern is consistent with previous studies showing that crop-raiding by macaques often occurs in forest-edge farms and fragmented landscapes (Priston and McLennan 2013; Koirala et al. 2022). Reported crop damage was concentrated in vegetable fields along the forest boundary (Table 7), with no evidence of

persistent conflict within residential areas during the study period. These crop-damage observations therefore provide contextual evidence of macaque use of agricultural edges, although crop types were not included as predictor variables in the MaxEnt model.

Habitat suitability modeling and environmental drivers

MaxEnt modeling demonstrated stable predictive performance across model replicates. Model complexity and parameterization were assessed using ENMeval based on cross-validated AUC, omission rate, and the Akaike Information Criterion corrected for small sample sizes (AICc). Among candidate models, the LQ feature class with a regularization multiplier of 4 yielded the lowest AICc ($\Delta AICc$: 0) and was selected as the final model. This model achieved a cross-validated AUC of 0.7469 ± 0.1023 with a low omission rate at the minimum training presence threshold (MTP: 0.0227), indicating stable discriminatory ability between relatively suitable and unsuitable environmental conditions (Table 8).

Analysis of predictor contributions revealed that habitat suitability for long-tailed macaques was primarily associated with disturbance-related predictors in the fitted model (Table 9). Distance to burned areas showed the highest contribution, followed by distance to settlements and land cover, together accounting for more than 90% of the total model contribution. Spatial predictions from the final MaxEnt model revealed a heterogeneous distribution of habitat suitability across the Mount Merbabu landscape (Figure 4).

The MTSS threshold (HSI: 0.558) derived from the cloglog output was applied to distinguish unsuitable from suitable environmental conditions. Using this threshold, 4,131.71 ha (25.80%) of the interaction-analysis area outside the national park (16,010.88 ha) was classified as suitable habitat, while 11,879.16 ha (74.20%) was classified as unsuitable. Suitable habitat was predicted not only within forested zones of Gunung Merbabu National Park but also across surrounding agricultural and settlement landscapes.

Response curves illustrate the relationships between key environmental predictors and predicted habitat suitability (Figure 5). The response pattern for distance to burned areas showed a non-linear relationship, with peak

suitability occurring at intermediate distances from burned areas. Other predictors exhibited more gradual response patterns, consistent with their relatively low contributions to overall model performance. Overall, these results show that disturbance-related variables, particularly distance to burned areas, emerged as the strongest predictors in the model. Based on these suitability patterns, the subsequent analysis focuses on delineating potential human-macaque spatial interaction zones by integrating habitat suitability thresholds with spatial constraints beyond the national park.

Delineation and robustness of spatial interaction zones

The delineation of potential human-macaque spatial interaction zones reveals pronounced spatial heterogeneity across landscapes surrounding GMNP. No interaction potential dominates the interaction-analysis area outside the national park, covering 11,879.16 ha and representing the majority of the mapped landscape (Figure 6, Table 10). These areas correspond to landscapes where predicted habitat suitability remains below the MTSS threshold, resulting in negligible spatial interaction potential. In contrast, moderate (3,511.44 ha) and high interaction potential zones (620.28 ha) are spatially limited and occur as localized clusters. Higher interaction zones are concentrated primarily along transitional areas between forest edges and surrounding agricultural and settlement landscapes rather than within forest interiors. The interaction zoning map shows that high interaction potential occurs along these forest-human interfaces, while moderate interaction zones form broader belts surrounding these cores.

Spatial extent by administrative units

At the district scale, the extent of spatial interaction zones varies among administrative areas (Table 10). No interaction potential zones account for the largest proportion of the landscape across all districts, whereas moderate and high interaction potential zones remain comparatively limited. Boyolali District contains the largest absolute extent of spatial interaction zones, with 1,853.47 ha of moderate interaction potential and 236.61 ha of high interaction potential. In contrast, Magelang District is overwhelmingly dominated by no interaction potential, with only 710.11 ha of moderate interaction potential and 62.20 ha of high interaction potential. Despite its smaller total area, Semarang District shows the highest proportional concentration of moderate to high spatial interaction zones, comprising 946.69 ha of moderate interaction potential and 321.47 ha

of high interaction potential. At a finer spatial scale, several villages show localized concentrations of moderate and high interaction zones (Table 11).

Spatial interaction zones across land-use types

Across land-use types, moderate to high interaction potential is concentrated mainly within agricultural and forest landscapes, with the forest category referring to forest patches located outside the national park boundary (Table 12). Agricultural land contains substantial portions of moderate interaction potential zones (1,362.46 ha), while forest areas account for the largest share of high interaction potential (461.04 ha). In contrast, built-up areas contribute minimally to high interaction potential (3.13 ha), whereas grassland areas display intermediate patterns, with 356.52 ha of moderate interaction potential and 34.85 ha of high interaction potential.

Table 7. Reported crop types damaged by long-tailed macaques in agricultural areas surrounding Gunung Merbabu National Park, Central Java, Indonesia

Crop type	Scientific name	Number of reports
Cabbage	<i>Brassica oleracea</i> var. <i>capitata</i>	36
Curly chili	<i>Capsicum annuum</i>	30
Broccoli	<i>Brassica oleracea</i> var. <i>italica</i>	25
Tobacco	<i>Nicotiana tabacum</i>	22
Carrot	<i>Daucus carota</i> subsp. <i>sativus</i>	22
Potato	<i>Solanum tuberosum</i>	17
Spring onion	<i>Allium fistulosum</i>	14
Celery	<i>Apium graveolens</i>	11
Mustard greens	<i>Brassica juncea</i>	8
Tomato	<i>Solanum lycopersicum</i>	7
Lettuce	<i>Lactuca sativa</i>	6
Shallot	<i>Allium cepa</i> var. <i>aggregatum</i>	6
Beet	<i>Beta vulgaris</i>	4
Cassava	<i>Manihot esculenta</i>	3
Maize	<i>Zea mays</i>	3
Bok coy	<i>Brassica rapa</i> subsp. <i>chinensis</i>	2
Slobor	<i>Brassica oleracea</i> var. <i>acephala</i>	2
Eggplant	<i>Solanum melongena</i>	1
Pumpkin	<i>Cucurbita moschata</i>	1
Sweet potato	<i>Ipomoea batatas</i>	1
Green bean	<i>Vigna radiata</i>	1
Snow pea	<i>Pisum sativum</i> var. <i>saccharatum</i>	1
Lotus	<i>Nelumbo nucifera</i>	1

Table 8. MaxEnt model selection results based on ENMeval

Feature class (FC)	RM	Δ AICc	AUC (mean \pm SD)	Omission rate (MTP)	No. parameters
LQ	4	0	0.7469 \pm 0.1023	0.0227	5
LQ	2.5	0.237	0.7454 \pm 0.1037	0.0227	6
LQ	3	0.973	0.7457 \pm 0.1033	0.0227	6
LQ	3.5	1.827	0.7466 \pm 0.1030	0.0227	6
LQH	3	1.999	0.7421 \pm 0.1072	0.0227	9

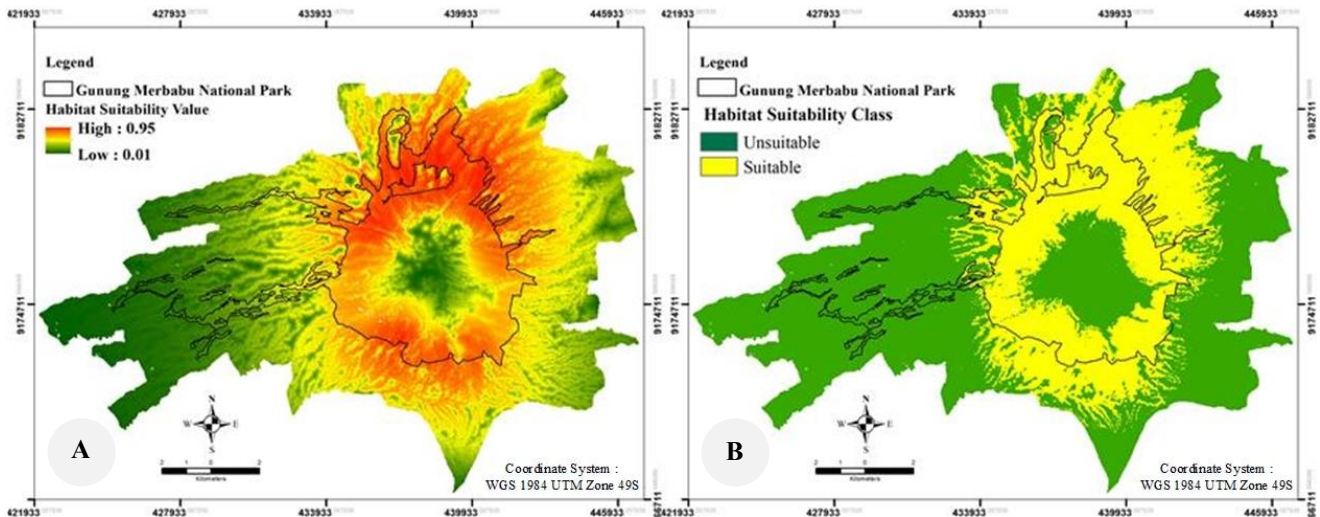


Figure 4. Habitat suitability of long-tailed macaques in the Mount Merbabu landscape: A. continuous habitat suitability index (HSI) predicted by the final MaxEnt model (cloglog scale), B. binary habitat classes derived using the MTSS threshold (HSI: 0.558). Based on this threshold, 11,879.16 ha (74.20%) of the area was classified as unsuitable and 4,131.71 ha (25.80%) as suitable, out of the interaction-analysis area (16,010.88 ha)

Table 9. Relative contribution of predictor variables in the MaxEnt model

Predictor variable	Percent contribution	Permutation importance
	(%)	(%)
Distance to burned areas (DistBurnArea)	74.3	64.9
Distance to settlements (DistSettle)	11.2	11.2
Land cover	7.7	0
Distance to dense forest (DistForest)	4	18
Distance to rivers (DistRiver)	2.6	4.9
Aspect	0.2	1
Slope	0	0
NDVI	0	0

Sensitivity and robustness of interaction models

Sensitivity analysis comparing the Comprehensive Occurrence (CO) and Indirect Occurrence Model (IOM) indicated comparable predictive performance. Both models produced similar mean AUC values (≈ 0.73 - 0.74), although the IOM exhibited higher omission rates and greater variance. Under the IOM model, moderate spatial interaction zones increased from 3,511.44 ha to 6,470.81 ha, while high spatial interaction zones expanded from 620.28 ha to 1,102.07 ha, indicating class transitions from moderate to high interaction in several areas. In the CO model, distance to burned areas was the dominant predictor, whereas the IOM model showed a stronger influence of distance to settlements, reflecting differences in occurrence data used for model calibration. The CO model was therefore retained as the primary analytical framework, while the IOM model served as a complementary sensitivity

model. Overall, the spatial distribution of interaction zones remained largely consistent between models, with differences mainly occurring in the classification of interaction potential levels.

Habitat suitability patterns in human-modified landscapes

Human-wildlife interactions in tropical landscapes often emerge where wildlife habitats overlap with expanding human land use (Mekonen 2020). Across many tropical regions, agricultural expansion and settlement development have transformed formerly continuous habitats into landscape mosaics composed of forests, agricultural land, and settlements, thereby increasing the likelihood of contact between humans and wildlife (Nyhus 2016; Sharma et al. 2020). Adaptable generalist species often persist in such heterogeneous landscapes, increasing encounter rates with humans (Nyhus 2016). In the Mount Merbabu landscape, habitat suitability modeling indicates that suitable habitat for long-tailed macaques extends beyond forested areas within Gunung Merbabu National Park into surrounding agricultural and settlement-dominated environments. The presence of suitable habitat within agricultural and settlement landscapes may therefore increase the likelihood of spatial interactions between macaques and local communities surrounding the national park. These spatial patterns are consistent with the ecological flexibility of long-tailed macaques as highly adaptable generalist primates capable of utilizing both natural and human-modified environments (Entezami et al. 2024). Similar patterns have been reported in other primate systems where suitable habitats extend beyond protected forests into human-influenced landscapes (Ji et al. 2022; Pramana et al. 2022).

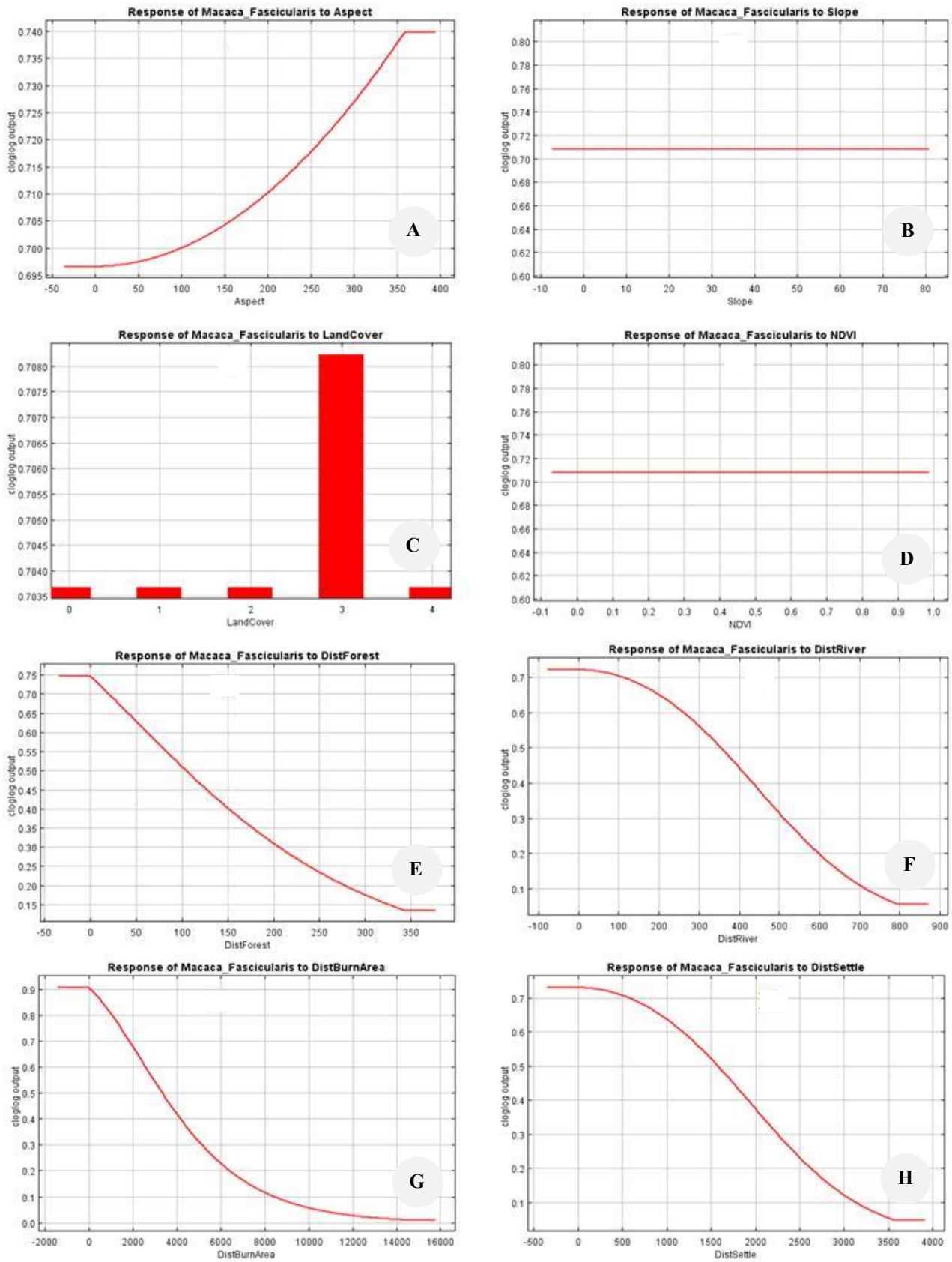


Figure 5. Response curves illustrating the relationships between habitat suitability and predictor variables. A. aspect, B. slope, C. land cover, D. NDVI, E. distance to rivers, F. distance to dense forest, G. distance to burned areas, H. distance to settlements

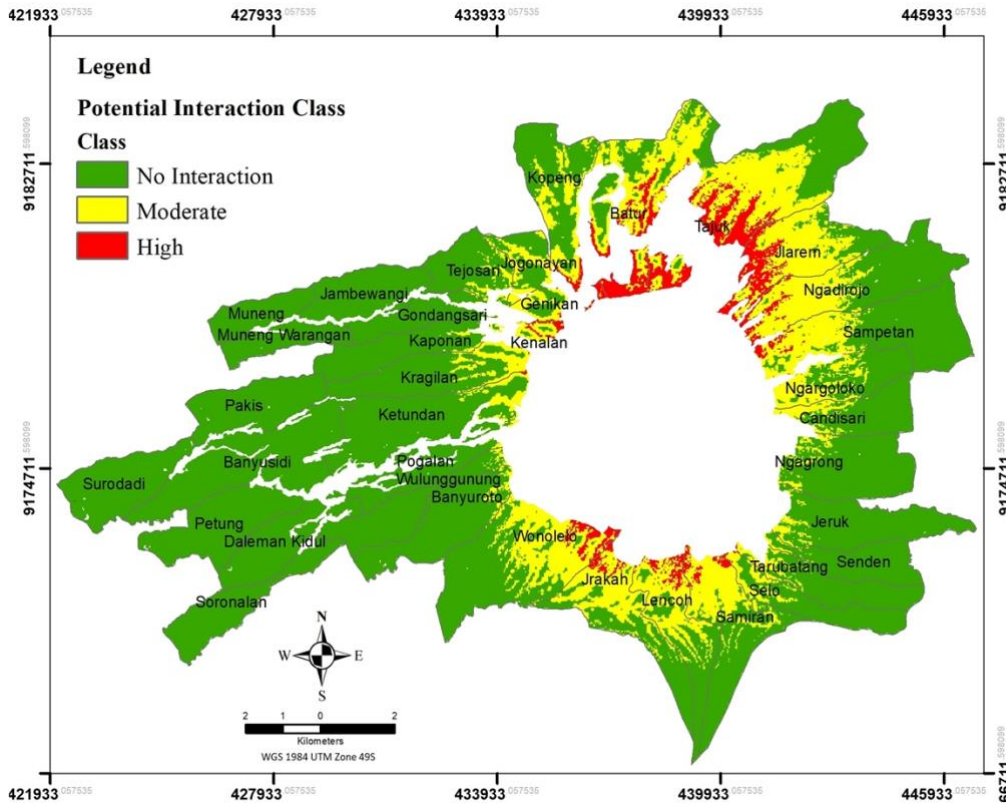


Figure 6. Spatial distribution of potential human-macaque interaction classes across villages surrounding the national park. Interaction potential was mapped within the interaction-analysis area outside the national park and classified into no interaction ($HSI < 0.558$), moderate interaction potential ($HSI: 0.558-0.808$), and high interaction potential ($HSI \geq 0.808$), based on habitat suitability thresholds derived from the final MaxEnt model using the Maximum Training Sensitivity plus Specificity (MTSS) criterion and the upper quartile (Q75) of predicted suitability

Table 10. Spatial extent of potential human-macaque interaction zones outside the national park by district

District	Spatial interaction potential			Total (ha)
	No interaction	Moderate (ha)	High (ha)	
Boyolali	4,053.50	1,853.47	236.61	6,143.58
Magelang	6,905.81	710.11	62.20	7,678.12
Semarang	907.28	946.69	321.47	2,175.44
Unclassified (no data)	12.57	1.17	-	13.74
Grand total	11,879.16	3,511.44	620.28	16,010.88

One of the key findings of this study is the strong contribution of disturbance-related variables, particularly distance to burned areas, as predictors of habitat suitability in the model. The spatial association between burned areas and predicted habitat suitability suggests that fire disturbance may be associated with macaque habitat use through changes in vegetation structure and the distribution of ecological resources (Santosa and Kwatrina 2020). This relationship should be interpreted as a spatial association rather than a direct ecological mechanism. The strong contribution of distance to burned areas may reflect broader disturbance gradients, including fire legacy effects, forest-edge dynamics, and landscape accessibility (Neves et al.

2020). Previous studies show that fire can modify habitat structure and landscape heterogeneity, influencing habitat use across multiple taxa (Nimmo et al. 2018; Neves et al. 2020). Therefore, the relationship between burned areas and habitat suitability observed in this study should be interpreted as an indirect signal of disturbance-related landscape dynamics rather than as direct evidence of post-fire ecological mechanisms.

The strong contribution of distance to burned areas may also partly reflect broader landscape gradients not explicitly represented in the model. In the Mount Merbabu landscape, large fires frequently originate near the forest-agriculture boundary where seasonal grass burning occurs during the dry season to stimulate vegetation regrowth in the following rainy season. When uncontrolled, fires can expand upslope into savanna areas with abundant fuel loads and strong wind exposure. Consequently, burned areas are often associated with forest edges, human land-use interfaces, and savanna vegetation dynamics. Accordingly, the distance-to-burned-area variable may function as a surrogate indicator of disturbance-related landscape gradients rather than representing a single ecological driver directly influencing macaque habitat use.

The response curves indicate a non-linear relationship between burned areas and habitat suitability, with peak suitability occurring at intermediate distances from burned

areas. These areas may represent transitional zones characterized by vegetation regeneration and increased landscape heterogeneity (Rossetti et al. 2024; Meneses et al. 2025). Habitat suitability declines at greater distances from burned areas, potentially reflecting increased proximity

to settlements and higher levels of human activity. These findings indicate that although long-tailed macaques are relatively adaptable to human-modified environments, their habitat use remains influenced by gradients of human disturbance and the availability of ecological resources.

Table 11. Area (ha) of potential human-macaque interaction classes for each village in the Mount Merbabu landscape, Central Java, Indonesia

District	Villages	Potential interaction class (Ha)			Grand total
		No interaction	Moderate	High	
Boyolali	Candisari	263.34	57.28	0.00	320.62
	Jeruk	460.01	30.63	0.00	490.64
	Jlarem	107.73	318.22	109.76	535.71
	Jrakah	262.06	233.51	20.40	515.98
	Lengoh	200.96	207.29	30.04	438.29
	Ngadirojo	391.57	278.77	31.57	701.92
	Ngagrong	489.58	36.72	0.00	526.30
	Ngargoloko	224.16	134.66	0.10	358.92
	Samiran	328.26	217.23	24.12	569.61
	Sampetan	513.55	222.20	17.87	753.62
	Selo	253.10	63.06	1.90	318.06
	Senden	280.00	11.50	0.00	291.51
	Tarubatang	279.19	42.39	0.83	322.42
Magelang	Banyuroto	457.17	19.76	0.00	476.93
	Banyusidi	711.21	0.00	0.00	711.21
	Daleman Kidul	339.21	0.00	0.00	339.21
	Genikan	39.26	46.64	2.54	88.45
	Gondangsari	218.10	2.89	0.00	220.99
	Jambewangi	329.59	0.00	0.00	329.59
	Jogonayan	109.64	72.79	0.40	182.83
	Kaponan	333.54	9.68	0.00	343.22
	Kenalan	59.98	106.13	13.01	179.13
	Ketundan	578.07	53.67	1.19	632.93
	Kragilan	323.33	21.04	0.00	344.37
	Muneng	202.28	0.00	0.00	202.28
	Muneng Warangan	205.05	0.00	0.00	205.05
	Pakis	389.52	0.00	0.00	389.52
	Petung	472.65	0.00	0.00	472.65
	Pogalan	259.40	7.18	0.00	266.58
	Soronalan	348.21	0.00	0.00	348.21
	Surodadi	419.88	0.00	0.00	419.88
	Tejosari	258.50	31.70	0.00	290.20
Wulunggunung	335.02	7.90	0.00	342.92	
Wonolelo	516.21	330.72	45.06	891.99	
Semarang	Batur	208.02	355.99	117.47	681.48
	Kopeng	350.76	135.80	22.55	509.12
	Tajuk	348.49	454.89	181.45	984.83
Unclassified (no data)		12.57	1.17	-	13.74
Grand total		11,879.16	3,511.44	620.28	16,010.88

Note: Interaction classes represent spatial interaction potential between human activities and macaque habitat suitability derived from spatial overlay analysis

Table 12. Spatial extent of potential human-macaque spatial interaction zones by land-use type outside the national park

Land use	Spatial interaction potential			
	No interaction (ha)	Moderate (ha)	High (ha)	Total (ha)
Built-up	1,206.66	139.31	3.13	1,349.10
Agriculture	5,682.80	1,362.46	121.26	7,169.52
Forest	4,107.64	1,651.98	461.04	6,220.66
Grassland	869.48	356.52	34.85	1,260.86
Unclassified (no data)	12.57	1.17	-	13.74
Grand total	11,879.16	3,511.44	620.28	16,010.88

Spatial configuration of human-macaque interaction zones

The delineation of spatial interaction zones suggests that potential human-macaque interactions may be spatially heterogeneous across the Mount Merbabu landscape. Most areas are characterized by no interaction potential, whereas moderate and high interaction zones were primarily predicted along forest-agriculture transition areas surrounding the national park boundary. This spatial configuration suggests that interaction potential is concentrated within specific landscape contexts rather than evenly distributed across the region. These mapped outputs should be interpreted primarily as relative prioritization surfaces for potential interaction zones rather than definitive ecological boundaries.

At district and village scales, variation in interaction potential reflects differences in landscape configuration rather than administrative boundaries. Areas with elevated interaction potential tend to occur where wildlife movement spaces intersect with agricultural land and settlement landscapes. Similar spatial patterns have been documented in other human-wildlife conflict systems, where interaction hotspots frequently emerge near conservation boundaries and ecotonal landscapes where ecological resources and human activities overlap (Koirala et al. 2022).

The distribution of spatial interaction zones across land-use types further supports this interpretation. Moderate to high interaction potential occurs primarily within agricultural and forest landscapes, whereas built-up areas contribute minimally to higher interaction potential. These patterns indicate that interaction potential emerges not simply from the presence of suitable habitat but from the spatial intersection of wildlife habitat, ecological disturbance, and human land use. Forest-agriculture transition zones, therefore, function as interaction-prone areas that simultaneously provide refuge for wildlife and access to anthropogenic food resources.

Management implications and study limitations

Management of human-macaque interactions should consider the degree of spatial overlap between wildlife habitats and agricultural landscapes. In areas classified as high interaction potential zones, mitigation strategies may focus on limiting macaque access to farmland through vegetation barriers and spatial crop arrangements that reduce the availability of preferred food resources. These strategies are proposed management options informed by previous studies and the mapped interaction patterns identified in this study, rather than interventions directly tested here. Mitigation efforts should also consider social aspects, including farmer perceptions and community participation, to enhance the effectiveness and acceptance of conflict management strategies (Depret and Sueur 2025). Modifying farm structure and crop placement has been suggested as a way to decrease the likelihood of primates entering cultivated fields (Hill 2000; Ueda et al. 2018). Landscape-based mitigation that reduces direct access to attractive crops is widely recognized as an effective non-lethal approach for managing human-wildlife conflict while maintaining conservation objectives (Nyhus 2016). In this context, arranging farmland in ecological buffer layers may

provide a practical approach to reducing conflict while maintaining habitat connectivity around protected areas. In areas classified as moderate interaction potential zones, management may prioritize reducing crop vulnerability based on preventive approaches suggested in previous human-wildlife conflict studies. The spatial distribution and seasonal availability of crops strongly influence primate crop-foraging behavior (Hill 2018). Increasing crop diversity and coordinating planting schedules among farmers may reduce both the spatial and temporal availability of preferred crops across agricultural landscapes (Tsuji and Ilham 2021). Collective planting strategies among farmers may therefore represent a potential community-based mechanism for reducing crop-raiding risk (Hill and Wallace 2012). In areas with no interaction potential, preventive management may help avoid future conflict escalation. Wildlife often becomes habituated to human environments when anthropogenic food resources are easily accessible (Dickman 2010). Proper waste management and the removal of food attractants near settlements may therefore prevent macaques from associating human landscapes with food rewards. Maintaining natural food availability within forest habitats may further reduce incentives for macaques to expand their foraging range into agricultural areas (Nyhus 2016). Maintaining clear ecological boundaries between forest habitats and human settlements may thus serve as an important preventive strategy for sustaining long-term coexistence between humans and wildlife.

Several limitations should be considered when interpreting these findings. Conflict data derived from community reports may be subject to reporting bias, as incidents are more likely to be recorded in accessible agricultural and settlement areas than in remote forest locations. Occurrence records were compiled from mixed detection sources, including field observations and community-reported incidents, and may therefore reflect both ecological patterns of macaque activity and spatial biases associated with human reporting opportunities. The absence of explicit social variables (such as human activity intensity, land-management practices, and community tolerance) also limits the model's ability to capture the social dimensions of human-macaque interactions. Temporal differences among environmental predictors may introduce additional uncertainty because burned-area data, land-cover variables, and occurrence records were derived from different years. In addition, the MaxEnt modeling framework relies on presence-only data and does not incorporate true absence records, which may influence model calibration and the interpretation of predicted suitability patterns. Furthermore, the delineation of interaction zones depends on operational threshold choices, including the MTSS threshold used to define suitable habitat and the upper quantile used to classify high interaction potential. Accordingly, the resulting interaction classes should be interpreted as relative spatial prioritization surfaces derived from model predictions rather than field-validated measures of conflict severity.

Future studies incorporating finer-scale social, behavioral, and seasonal resource availability data would improve the predictive accuracy of spatial interaction models and enhance

their relevance for adaptive wildlife management in human-dominated landscapes. Overall, this study demonstrates how spatial modeling of habitat suitability and interaction zones can reveal the landscape processes shaping human-wildlife encounters. By identifying where ecological disturbance, wildlife habitat, and human land use intersect, this approach provides a spatially explicit basis for proactive coexistence strategies in protected-area buffer zones and other human-dominated landscapes.

In conclusion, this study identifies spatial interaction zones between humans and long-tailed macaques across the Mount Merbabu landscape, with interaction potential concentrated primarily along forest-agriculture transition areas surrounding the national park. Habitat suitability modeling indicates that distance to burned areas is the strongest predictor shaping macaque occurrence patterns within the study landscape. By integrating habitat suitability with land-use patterns outside the protected area, the resulting spatial interaction map provides a practical basis for spatially targeted mitigation, including strengthened crop protection in high-interaction zones, preventive edge management in moderate zones, and monitoring in low-interaction areas. However, these mapped zones represent relative spatial interaction potential derived from model predictions, rather than direct measures of conflict occurrence or severity. Accordingly, the results should be interpreted as spatial prioritization surfaces that support adaptive management while acknowledging the ecological and social uncertainties inherent in predictive spatial modeling.

ACKNOWLEDGEMENTS

We are deeply grateful to the Gunung Merbabu National Park Authority, the Ministry of Forestry of the Republic of Indonesia, and the Forestry Management Study Program, Faculty of Agriculture, Universitas Sebelas Maret, for their support in conducting this study. We also extend our sincere appreciation to the data collection team: Ekowati Murwaningsih, Hendro Prasajo, Ayu Kurnia Aissiyah, Eko Yuwono, Efiyati, Endah Ratnaningrum, Dejan Shaka Juang, Fatikha Ryadiyan Sari, and Anifah Fatimatul Jannah.

REFERENCES

- Aissiyah AK, Faida LRW, Hermawan MTT. 2019. Pemanfaatan rumput dan kayu bakar untuk kebutuhan subsisten masyarakat di Taman Nasional Gunung Merbabu. *Jurnal Manusia Lingkungan* 26: 20-27. <https://doi.org/10.22146/jml.23635>. [Indonesian]
- Anand S, Radhakrishna S. 2017. Investigating trends in human-wildlife conflict: Is conflict escalation real or imagined? *J Asia-Pac Biodiv* 10: 154-161. <https://doi.org/10.1016/j.japb.2017.02.003>.
- Ardiaristo A, Prasetyo LB, Syaufina L, Kosmaryandi N. 2024. Monitoring vegetation changes and disturbances in Gunung Merbabu National Park using LandTrendr algorithm and Landsat images. *Ecol Eng Environ Technol* 25: 298-307. <https://doi.org/10.12912/27197050/188872>.
- Badan Informasi Geospasial. 2019. Peta Rupabumi Indonesia (RBI). Badan Informasi Geospasial, Cibinong, Indonesia. [Indonesian]
- Chai SL, Zhang J, Nixon A, Nielsen S. 2016. Using risk assessment and habitat suitability models to prioritize invasive species for management in a changing climate. *PLoS One* 11 (10): e0165292. <https://doi.org/10.1371/journal.pone.0165292>.
- Depret M, Sueur C. 2025. Management of coexistence and conflicts between humans and macaques in Japan. *Animals* 15 (7): 888. <https://doi.org/10.3390/ani15070888>.
- Dewi K, Hardian AS, Cahyono SA. 2024. Assessing the economic value of water environmental services in Mount Merbabu National Park. *Jurnal Sylva Lestari* 12 (2): 338-352. <https://doi.org/10.23960/jsl.v12i2.802>.
- Dickman AJ. 2010. Complexities of conflict: The importance of considering social factors in human-wildlife conflict. *Anim Conserv* 13: 458-466. <https://doi.org/10.1111/j.1469-1795.2010.00368.x>.
- Dormann CF, Elith J, Bacher S, Buchmann C, Carl G, Carré G, Marquéz JRG, Gruber B, Lafourcade B, Leitão PJ, Münkemüller T, McClean C, Osborne PE, Reineking B, Schröder B, Skidmore AK, Zurell D, Lautenbach S. 2013. Collinearity: A review of methods to deal with it and a simulation study evaluating their performance. *Ecography* 36: 27-46. <https://doi.org/10.1111/j.1600-0587.2012.07348.x>.
- Elith J, Phillips SJ, Hastie T, Dudik M, Chee YE, Yates CJ. 2011. A statistical explanation of MaxEnt for ecologists. *Divers Distrib* 17: 43-57. <https://doi.org/10.1111/j.1472-4642.2010.00725.x>.
- Entezami M, Mustaqqim F, Morris E, Swee E, Lim H, Prada M, Paramasivam SJ. 2024. Effect of human activity and presence on the behavior of long-tailed macaques (*Macaca fascicularis*) in an urban tourism site in Kuala Selangor, Malaysia. *Animals* 14 (8): 1173. <https://doi.org/10.3390/ani14081173>.
- EROS Center. 2020. Landsat 8 Operational Land Imager (OLI) Collection 2 Level-2 Science Products. USGS Earth Resources Observation and Science (EROS) Center. Sioux Falls, USA.
- European Space Agency. 2021. Sentinel-2 Level-2A Surface Reflectance Data Product. European Space Agency (ESA), France. <https://scihub.copernicus.eu/>.
- Esthi RB, Irawan NC, Setiawan I. 2022. The nexus between ecological competence, forest area management, and sustainable agroecosystem performance for communities around Mount Merbabu National Park (MMbNP). *IOP Conf Ser Earth Environ Sci* 1108 (1): 012019. <https://doi.org/10.1088/1755-1315/1108/1/012019>.
- Fadhillah DN. 2020. Identifikasi aves di kawasan Taman Nasional Gunung Merbabu sebagai bahan pembuatan multimedia interaktif biologi SMA. *J Biol Learn* 2 (1): 50-57. <https://doi.org/10.32585/v2i1.832>. [Indonesian]
- Farr TG, Rosen PA, Caro E, Crippen R, Duren R, Hensley S, Kobrick M, Paller M, Rodriguez E, Roth L, Seal D, Shaffer S, Shimada J, Umland J, Werner M, Oskin M, Burbank D, Alsdorf D. 2007. The shuttle radar topography mission. *Rev Geophys* 45: RG2004. <https://doi.org/10.1029/2005RG000183>.
- Fauzi R, Wuryanto T, Endarto, Suarmadi F, Tomono B. 2020. Distribution of long-tailed macaque (*Macaca fascicularis*) in Kelimutu National Park. *IOP Conf Ser Earth Environ Sci* 591: 012041. <https://doi.org/10.1088/1755-1315/591/1/012041>.
- Fitria W, Bambang AN, Hidayat JW. 2020. Human and long-tailed macaque conflict in Central Java, Indonesia. *E3S Web Conf* 202: 06011. <https://doi.org/10.1051/e3sconf/202020206011>.
- Fratesi A, Di E, Briefer EF, Nielsen DRK. 2026. "Monkey influencers": Conservation culturomics of human-macaque (*Macaca fascicularis*) interactions. *Glob Ecol Conserv* 65: e04016. <https://doi.org/10.1016/j.gecco.2025.e04016>.
- Hill CM. 2000. Conflict of interest between people and baboons: Crop raiding in Uganda. *Intl J Primatol* 21: 299-315. <https://doi.org/10.1023/A:1005481605637>.
- Hill CM, Wallace GE. 2012. Crop protection and conflict mitigation: Reducing the costs of living alongside non-human primates. *Biodivers Conserv* 21: 2569-2587. <https://doi.org/10.1007/s10531-012-0318-y>.
- Hill CM. 2018. Crop foraging, crop losses, and crop raiding. *Annu Rev Anthropol* 47: 377-394. <https://doi.org/10.1146/annurev-anthro-102317-050022>.
- Ji Y, Wei X, Liu F, Li D, Li J. 2022. Spatial-temporal patterns of human-wildlife conflicts under coupled impact of natural and anthropogenic factors in Mt. Gaoligong, western Yunnan, China. *Glob Ecol Conserv* 40: e02329. <https://doi.org/10.1016/j.gecco.2022.e02329>.
- Johnson CL, Hilsner H, Linkie M, Rahasia R, Rovero F, Pusparini W, Hunowu I, Patandung A, Andayani N, Tasirin J, Nistyantara LA, Bowkett AE. 2020. Using occupancy-based camera-trap surveys to assess the critically endangered primate *Macaca nigra* across its

- range in North Sulawesi, Indonesia. *Oryx* 54 (6): 784-793. <https://doi.org/10.1017/S0030605319000851>.
- Kass JM, Muscarella R, Galante PJ, Bohl CL, Pinilla-Buitrago GE, Soley-Guardia M, Anderson RP. 2021. ENMeval 2.0: Redesigned for customizable and reproducible modeling of species' niches and distributions. *Methods Ecol Evol* 12: 1602-1608. <https://doi.org/10.1111/2041-210X.13628>.
- Koirala S, Baral S, Garber PA, Basnet H, Bahadur H, Gurung S, Rai D, Gaire R, Sharma B, Pun T, Li M. 2022. Identifying the environmental and anthropogenic causes, distribution, and intensity of human rhesus macaque conflict in Nepal. *J Environ Manag* 316: 115276. <https://doi.org/10.1016/j.jenvman.2022.115276>.
- Larson KL, Rosales Chavez JB, Brown JA, Morales-Guerrero J, Avilez D. 2023. Human-wildlife interactions and coexistence in an urban desert environment. *Sustainability* 15 (4): 3307. <https://doi.org/10.3390/su15043307>.
- Lee SH, Lee MH, Kang TH, Cho HR, Yun HS, Lee SJ. 2025. Comparative analysis of dNBR, dNDVI, SVM kernels, and ISODATA for wildfire-burned area mapping using Sentinel-2 imagery. *Remote Sens* 17 (13): 2196. <https://doi.org/10.3390/rs17132196>.
- Li X, Wang Z, Wang S, Qian Z. 2024. MaxEnt and Marxan modeling to predict the potential habitat and priority planting areas of *Coffea arabica* in Yunnan, China under climate change scenario. *Front Plant Sci* 15: 1471653. <https://doi.org/10.3389/fpls.2024.1471653>.
- Matseketsa G, Muboko N, Gandiwa E, Kombora DM. 2019. An assessment of human-wildlife conflicts in local communities bordering the western part of Save Valley. *Glob Ecol Conserv* 20: e00737. <https://doi.org/10.1016/j.gecco.2019.e00737>.
- Mekonen S. 2020. Coexistence between human and wildlife: The nature, causes and mitigations of human-wildlife conflict around Bale Mountains National Park, Southeast Ethiopia. *BMC Ecol* 20: 51. <https://doi.org/10.1186/s12898-020-00319-1>.
- Meneses OM, Ribeiro NS, Shirvani Z. 2025. Resilience of the Miombo woodland to different fire frequencies in the LevasFlor Forest Concession, central Mozambique. *Forests* 16 (1): 10. <https://doi.org/10.3390/f16010010>.
- Mishra PS, Kumara HN, Thiyagesan K, Singh M, Velankar AD, Pal A. 2020. Chaos in coexistence: Perceptions of farmers towards long-tailed macaques related to crop loss on Great Nicobar Island. *Primate Conserv* 34: 175-183.
- Muscarella R, Galante PJ, Soley-Guardia M, Boria RA, Kass JM, Anderson RP. 2014. ENMeval: An R package for conducting spatially independent evaluations and estimating optimal model complexity for MaxEnt ecological niche models. *Methods Ecol Evol* 5: 1198-1205. <https://doi.org/10.1111/2041-210X.12261>.
- Neves MB, Chiarani E, Ferreira MP, Fontana CS. 2020. The role of fire disturbance on habitat structure and bird communities in South Brazilian Highland grasslands. *Sci Rep* 10: 19708. <https://doi.org/10.1038/s41598-020-76758-z>.
- Nimmo DG, Avitabile S, Banks SC, Bliege-Bird R, Callister K, Clarke MF, Dickman CR, Doherty TS, Driscoll DA, Greenville AC, Haslem A, Kelly LT, Kenny SA, Lahoz-Monfort JJ, Lee C, Leonard S, Moore H, Newsome TM, Parr CL, Ritchie EG, Schneider K, Turner JM, Watson S, Westbrooke M, Wouters M, White M, Bennett AF. 2018. Animal movements in fire-prone landscapes. *Biol Rev* 94: 981-998. <https://doi.org/10.1111/brv.12486>.
- Nyhus PJ. 2016. Human-wildlife conflict and coexistence. *Annu Rev Environ Resour* 41: 143-171. <https://doi.org/10.1146/annurev-environ-110615-085634>.
- Osman A, Mariwah S, Yawson DO, Atampugre G. 2022. Changing land cover and small mammal habitats: Implications for landscape ecological integrity. *Environ Chall* 7: 100514. <https://doi.org/10.1016/j.envc.2022.100514>.
- Pérez-Cutillas P, Pérez-Navarro A, Conesa-García C, Zema DA, Amado-Álvarez JP. 2023. What is going on within Google Earth Engine? A systematic review and meta-analysis. *Remote Sens Appl Soc Environ* 29: 100907. <https://doi.org/10.1016/j.rsase.2022.100907>.
- Phillips SJ, Anderson RP, Schapire RE. 2006. Maximum entropy modeling of species geographic distributions. *Ecol Model* 190: 231-259. <https://doi.org/10.1016/j.ecolmodel.2005.03.026>.
- Phillips SJ, Dudík M. 2008. Modeling of species distributions with MaxEnt: New extensions and a comprehensive evaluation. *Ecography* 31: 161-175. <https://doi.org/10.1111/j.0906-7590.2008.5203.x>.
- Phillips SJ, Dudík M, Elith J, Graham CH, Lehmann A, Leathwick J, Ferrier S. 2009. Sample selection bias and presence-only distribution models: implications for background and pseudo-absence data. *Ecol Appl* 19: 181-197. <https://doi.org/10.1890/07-2153.1>.
- Pramana GTS, Prasetyo LB, Iskandar E. 2022. The habitat suitability modelling of dare monkey (*Macaca maura*) in Bantimurung Bulusaraung National Park, South Sulawesi. *J Nat Resour Environ Manag* 13 (1): 57-67. <https://doi.org/10.29244/jpsl.13.1.57-67>.
- Priston NEC, McLennan MR. 2013. Managing humans, managing macaques: Human-macaque conflict in Asia and Africa. In: Radhakrishna S, Huffman MA, Sinha A (eds). *The Macaque Connection: Cooperation and Conflict between Humans and Macaques*. Springer, New York.
- Rifaie F, Sulistyadi E, Sulistya Y, Inayah N. 2024. Spatial patterns of human long-tailed macaque (*Macaca fascicularis*) conflicts in Java Island: A comparison of two secondary data sources. *J Asia-Pac Biodiv* 17 (4): 653-662. <https://doi.org/10.1016/j.japb.2024.05.008>.
- Rossetti I, Calderisi G, Cogoni D. 2024. Post-fire vegetation (non-) recovery across the edges of a wildfire: An unexplored theme. *Fire* 7 (7): 250. <https://doi.org/10.3390/fire7070250>.
- Safanelli L, Poppell RR, Ruiz CF, Bonfatti BR, Alcantara F, Mello DO, Rizzo R. 2020. Terrain analysis in Google Earth Engine: A method adapted for high-performance global-scale analysis. *ISPRS Intl J Geo-Inf* 9 (6): 400. <https://doi.org/10.3390/ijgi9060400>.
- Santosa Y, Kwatrina RT. 2020. Effect of forest fire on mammals: Comparisons of species diversity across different time periods and areas. *IOP Conf Ser Earth Environ Sci* 528: 012023. <https://doi.org/10.1088/1755-1315/528/1/012023>.
- Sari DR, Hadi M, Rahadian R. 2018. Kelimpahan dan keanekaragaman kupu-kupu di kawasan Taman Nasional Gunung Merbabu, Jawa Tengah. *Bioma* 18 (2): 173-179. <https://doi.org/10.14710/bioma.18.2.173-179>. [Indonesian]
- Savitri R, Mukhtar AS, Iskandar S. 2010. Status konservasi mamalia dan burung di Taman Nasional Merbabu (Mammals and aves conservation status in Merbabu National Park). *Jurnal Penelitian Hutan dan Konservasi Alam* 7 (3): 227-239. [Indonesian]
- Schroeder W, Oliva P, Giglio L, Csizsar IA. 2014. The new VIIRS 375 m active fire detection data product: Algorithm description and initial assessment. *Remote Sens Environ* 143: 85-96. <https://doi.org/10.1016/j.rse.2013.12.008>.
- Sharma P, Chettri N, Uddin K, Wangchuk K. 2020. Mapping human-wildlife conflict hotspots in a transboundary landscape, Eastern Himalaya. *Glob Ecol Conserv* 24: e01284. <https://doi.org/10.1016/j.gecco.2020.e01284>.
- Soulsbury A, White PCL. 2015. Human-wildlife interactions in urban areas: A review of conflicts, benefits and opportunities. *Wildl Res* 42: 541-553. <https://doi.org/10.1071/WR14229>.
- Syah MJ. 2020. Long-tailed macaques (*Macaca fascicularis*) and humans interactions in Grojogan Sewu Natural Park, Karanganyar Regency, Central Java Province. *Al-Hayat J Biol Appl Biol* 3 (1): 31-36. <https://doi.org/10.21580/ah.v3i1.6069>.
- Syahran FN, Rahman DA, Santosa Y. 2025. Habitat-based spatial prediction of human-elephant conflict risk in Sumatra. *Biodiversitas* 26 (9): 4465-4478. <https://doi.org/10.13057/biodiv/d260919>.
- Tang J, Chen Z, Yin X, Teng J, Gao W, Liu Y, Li X. 2025. Species richness prediction and priority conservation planning for rare *Michelia* species in China. *Sci Rep* 15: 11025. <https://doi.org/10.1038/s41598-025-11025-7>.
- Tsuji Y, Ilham K. 2021. Studies on primate crop feeding in Asian regions: A review. *Mamm Stud* 46 (2): 97-113. <https://doi.org/10.3106/ms2020-0043>.
- Ueda Y, Kiyono M, Nagano T, Mochizuki S, Murakami T. 2018. Damage control strategies affecting crop-raiding Japanese macaque behaviors in a farming community. *Hum Ecol* 46 (2): 259-268. <https://doi.org/10.1007/s10745-018-9972-3>.
- Wu Q, Dai Y, Sun Q. 2024. Human-wildlife conflict patterns and hotspot prediction in the southern foothills of the Qinling Mountains, China. *Front Ecol Evol* 12: 1435811. <https://doi.org/10.3389/fevo.2024.1435811>.
- Yeo J, Neo H. 2010. Monkey business: Human-animal conflicts in urban Singapore. *Soc Cult Geogr* 11: 681-699. <https://doi.org/10.1080/14649365.2010.508565>.
- Zvidzai M, Mawere KK, Rodney JN, Ndaimani H, Zanamwe C, Zengeya FM. 2023. Application of maximum entropy (MaxEnt) to understand the spatial dimension of human-wildlife conflict risk in areas adjacent to Gonarezhou National Park, Zimbabwe. *Ecol Soc* 28: 18. <https://doi.org/10.5751/ES-14420-280318>.